Journal of Energetic Materials
Publication details, including instructions for authors and subscription information:
http://www.informaworld.com/smpp/title~content=t713770432

Effects of Endothermic Binders on Times to Explosion of HMX- and TATB-Based Plastic Bonded Explosives

Craig M. Tarver[a]; Jake G. Koerner[a]
[a] Energetic Materials Center, Lawrence Livermore National Laboratory, Livermore, California, USA

To cite this Article Tarver, Craig M. and Koerner, Jake G.(2008) 'Effects of Endothermic Binders on Times to Explosion of HMX- and TATB-Based Plastic Bonded Explosives', Journal of Energetic Materials, 26: 1, 1 — 28
To link to this Article: DOI: 10.1080/07370650701719170
URL: http://dx.doi.org/10.1080/07370650701719170

Journal of Energetic Materials, 26: 1–28, 2008

ISSN: 0737-0652 print/1545-8822 online
DOI: 10.1080/07370650701719170

Taylor & Francis
Taylor & Francis Group

Effects of Endothermic Binders on Times to Explosion of HMX- and TATB-Based Plastic Bonded Explosives

CRAIG M. TARVER
JAKE G. KOERNER

Energetic Materials Center, Lawrence Livermore National Laboratory, Livermore, California, USA

Plastic-bonded explosives (PBXs) based on octahydro-1,3,5,7-tetranitro-1,3,5,7-tetrazocine (HMX) or 1,3,5-triamino-2,4,6-trinitrobenzene (TATB) formulated with the endothermic binders Estane, Viton, or Kel-F exhibit longer times to thermal explosion than do pure HMX and TATB in the one-dimensional time to explosion (ODTX) and in other thermal experiments. Previous chemical kinetic thermal decomposition models for HMX- and TATB- based PBXs assumed that the binders decomposed independently of and at lower temperatures than the explosives. Recent chemical decomposition rate measurements showed that Estane, Viton, and Kel-F are more thermally stable than HMX and TATB. Thus, the longer thermal explosion times for these PBXs are most likely due to endothermic decompositions of the binders by reactions with the gaseous decomposition products of HMX and TATB. New PBX chemical decomposition models are developed using the global HMX and TATB models, measured binder kinetics, and cross-reactions between gaseous explosive products and binders. These new models accurately predict ODTX time to explosion and other experimental data.

Address correspondence to Craig M. Tarver, Energetic Materials Center, L-282, Lawrence Livermore National Laboratory, P.O. Box 808, Livermore, CA 94551, USA. E-mail: tarver1@llnl.gov

Keywords: endothermic binders, HMX, TATB, thermal explosion

Introduction

Plastic-bonded explosives (PBXs) based on octahydro-1,3,5,7-tetranitro-1,3,5,7-tetrazocine (HMX) or 1,3,5-triamino-2,4,6-trinitrobenzene (TATB) are often formulated with endothermic binders to improve their mechanical and thermal properties [1]. PBXs of HMX and TATB formulated with Estane, Viton A, and Kel-F 800 exhibit longer times to thermal explosion than pure HMX and TATB in one-dimensional time to explosion (ODTX) and other thermal explosion experiments [2]. Chemical decomposition models were developed to predict times to explosion and the locations within the explosive charges where runaway reactions first occur [2–4]. These predictions are used as the basis for estimations of the violence of thermal explosions as functions of heating rate, confinement, damage, and porosity [5,6]. Since little experimental chemical kinetic data have been obtained at higher temperatures, these models have been used to predict the times to explosion measured in high-power laser heating experiments [7]; estimate the critical conditions for ''hot-spot'' ignition during impact and shock compression scenarios [8]; and model the growth rates of shock-induced hot spots during shock-to-detonation transition (SDT) processes [9]. They are used to model shock initiation and detonation wave propagation in the statistical hot spot reactive flow model in the thermal-mechanical-hydrodynamic–coupled computer code ALE3D [10].

Burnham and Weese [11] measured the thermal degradation kinetics of three endothermic binders used in PBXs: Estane 5703 P, a poly(ester urethane) block copolymer; Viton A, a vinylidene-hexafluoropropene copolymer; and Kel-F 800, a vinylidene-chlorotrifluorethene copolymer. Simultaneous differential thermogravimetric analysis was conducted at several heating rates to obtain percentage of decomposition versus temperature data. These experiments showed that Estane, Viton A, and Kel-F are more thermally stable than HMX and TATB.

Previous chemical reaction models for HMX and TATB PBXs assumed that the binders decomposed independently of and at lower temperatures than the explosive particles. The new binder kinetic data suggest that endothermic degradation of the binders by gaseous explosive decomposition products as they are produced causes the measured longer times to explosion for the PBXs. To test this hypothesis, ''cross-reactions'' between the binders that cover the explosive particles and the evolving HMX and TATB gaseous decomposition products are added to the thermal decomposition models. The calculated times to explosion for these PBX models are compared to ODTX and other experimental measurements for several PBXs.

Chemical Kinetic Decomposition Models for HMX and TATB

Three to five step global chemical decomposition models have been developed for several solid high explosives. The HMX chemical decomposition model consists of four reactions and five chemical species. The reaction sequence is [4]:

$$\text{Beta HMX} \rightarrow \text{Delta HMX} \tag{1}$$

$$\text{Delta HMX} \rightarrow \text{Solid Intermediates} \tag{2}$$

$$\text{Solid Intermediates} \rightarrow \text{Gaseous Intermediates} \quad (\text{CH}_2\text{O},\ \text{N}_2\text{O},\ \text{HCN},\ \text{HNO}_2, \ldots) \tag{3}$$

$$\text{Gaseous Intermediates} \rightarrow \text{Final Products} \quad (\text{CO}_2, \text{H}_2\text{O}, \text{N}_2, \text{CO}, \text{C}, \ldots) \tag{4}$$

The major pathways for HMX decomposition have been reviewed by Behrens et al. [12]. The solid-solid beta to delta phase transition is treated as a separate reaction in Eq. (1) [4], whereas previously it had been included in Eq. (2) as one overall endothermic process [2]. Equation (2) describes the initial ring- and bond-breaking endothermic step(s). HMX decomposition is known to produce mainly CH_2O plus N_2O under some temperature and pressure conditions and mainly HCN plus HNO_2 under other conditions [12]. Equation (3) is

slightly exothermic, and thus most of HMX's chemical energy is released during the gas phase formation of the final stable reaction products such as CO_2, CO, N_2, and H_2O by second-order gas phase reactions represented by Eq. (4).

The TATB model is based on less chemical kinetic data than the HMX model [5]. It consists of three reactions and four species. The TATB sequence is

$$\text{TATB} \rightarrow \text{Solid Intermediate A} + H_2O \quad (5)$$

$$\text{Solid Intermediate A} \rightarrow \text{Solid Intermediate B} + \text{Gases} \quad (6)$$

$$\text{Solid Intermediate B} \rightarrow \text{Final gaseous products} \quad (7)$$

It is known that TATB reacts mainly in the condensed phase and that all of the possible H_2O molecules can be formed during extremely slow heating, leaving $C_6N_6O_3$ behind [5]. At faster heating rates, the first two reactions, Eq. (5) and (6), are assumed to be endothermic steps that eliminate H_2O and then form other intermediate gaseous products, such as NO. The third reaction is assumed to be an exothermic, second-order reaction. Some experimental kinetic data are available for the rates of the three reactions [5]. In the ODTX apparatus, heavily confined and unconfined TATB-based explosives exhibit essentially the same times to explosion [2,5]. Thus, gas phase reactions do not dominate the chemical energy release process in TATB as they do in HMX. This fact is borne out by the successful modeling of unconfined TATB laser heating experiments [7].

Tables 1 and 2 list the thermal property and reaction rate parameters for the HMX and TATB decomposition models, respectively. Both models have been used in the Chemical TOPAZ heat transfer code [13] to calculate times to and locations of thermal explosion for the ODTX experiment and for other thermal experiments with various heating rates, degrees of confinement, and geometries.

Chemical Kinetic Decomposition Models for Binders and PBXs

The three endothermic binders were heated at rates varying from 0.2°C per minute to 40°C per minute, and their weight

Table 1
Thermal and reaction rate parameters for the HMX model

	Beta HMX	Delta HMX	Solid intermediate	Intermed. gases	Final gases
1. Initial Density (g/cm^3)					
	1.85	1.70			
2. Heat capacity (cal/g-K) at:					
298 K	0.24	0.24	0.22	0.24	0.27
373 K	0.30	0.30	0.27	0.26	0.28
433 K	0.34	0.34	0.31	0.27	0.28
563 K	0.40	0.40	0.36	0.29	0.29
623 K	0.46	0.46	0.42	0.31	0.30
773 K	0.55	0.55	0.50	0.35	0.31
1273 K	0.55	0.55	0.50	0.42	0.35
3. Thermal conductivity (cal/cm-g-K) at:					
298 K	1.28×10^{-3}	1.18×10^{-3}	1.08×10^{-3}	9.80×10^{-4}	1.0×10^{-4}
373 K	1.09×10^{-3}	1.00×10^{-3}	9.20×10^{-4}	8.80×10^{-4}	1.0×10^{-4}
433 K	1.02×10^{-3}	9.20×10^{-4}	8.30×10^{-4}	8.30×10^{-4}	1.0×10^{-4}
563 K	8.15×10^{-4}	8.15×10^{-4}	8.15×10^{-4}	8.15×10^{-4}	1.0×10^{-4}
623 K	7.50×10^{-4}	7.50×10^{-4}	7.50×10^{-4}	7.50×10^{-4}	1.0×10^{-4}

(*Continued*)

Table 1
Continued

	Beta HMX	Delta HMX	Solid intermediate	Intermed. gases	Final gases
773 K	1.00×10^{-4}	1.00×10^{-4}	1.00×10^{-4}	1.00×10^{-4}	1.0×10^{-4}
>1273 K	1.00×10^{-4}	1.00×10^{-4}	1.00×10^{-4}	1.00×10^{-4}	1.0×10^{-4}
4. Heat of formation (cal/g)					
	+61.0	+71.0	+131.0	−2.0	−1339.0

5. Reaction rate parameters $Na^{x}qZ\ e^{-E/RT}$(where Na is mass fraction)

Reaction	ln Z	E(kcal/mol)	Reaction order x	Heat of reaction q(cal/g)
1	48.13	48.47	1	+10.0
2	48.7	52.70	1	+60.0
3	37.8[a]	44.30	1	−133.0
4	28.1[b]	34.10	2	−1337.0

[a] 38.23 for fine HMX particles; [b]28.53 for fine HMX particles.

Table 2
Thermal and reaction rate parameters for the TATB model

	TATB	Solid intermediate A	Solid intermediate B	Gaseous products
1. Initial density (g/cm^3) = 1.835 g				
2. Heat capacity (cal/g-K) at:				
298 K	0.26	0.24	0.26	0.26
433 K	0.36	0.33	0.28	0.28
573 K	0.45	0.39	0.29	0.29
623 K	0.47	0.41	0.30	0.30
673 K	0.49	0.42	0.30	0.30
773 K	0.54	0.48	0.35	0.35
>1273 K	0.54	0.48	0.35	0.35
3. Thermal conductivity (cal/cm-g-K) at:				
298 K	2.10×10^{-3}	1.05×10^{-3}	5.00×10^{-4}	1.00×10^{-4}
433 K	1.56×10^{-3}	7.80×10^{-4}	3.90×10^{-4}	1.00×10^{-4}
573 K	1.10×10^{-3}	5.50×10^{-4}	2.70×10^{-4}	1.00×10^{-4}
623 K	1.00×10^{-3}	5.00×10^{-4}	2.50×10^{-4}	1.00×10^{-4}
673 K	1.00×10^{-3}	1.00×10^{-4}	1.00×10^{-4}	1.00×10^{-4}
773 K	1.00×10^{-4}	1.00×10^{-4}	1.00×10^{-4}	1.00×10^{-4}
>1273 K	1.00×10^{-4}	1.00×10^{-4}	1.00×10^{-4}	1.00×10^{-4}

(*Continued*)

Table 2
Continued

	TATB	Solid intermediate A	Solid intermediate B	Gaseous products
4. Heat of formation (cal/g)				
	−142.7	−92.7	+42.7	−742.7
5. Reaction rate parameters $Na^{x}qZ\ e^{-E/RT}$(where Na is mass fraction)				
Reaction	ln Z	E(kcal/mol)	Reaction order x	Heat of reaction q(cal/g)
1	48.0	60.0	1	+50.0
2	29.8[a]	42.0	1	+50.0
3	26.8[b]	33.8	2	−700.0

[a] 30.8 for ultrafine TATB particles; [b] 27.8 for ultrafine TATB particles.

losses versus time and temperature were measured [11]. The resulting curves were then used to determine Arrhenius rate parameters. Estane is the least stable of the three binders and Viton A the most stable, although Kel-F's stability is similar to that of Viton A. Viton A and Kel-F exhibited primarily a single reaction rate, while Estane appeared to have two reaction rate components with a rate change occurring at 42% decomposition. Table 3 lists the room-temperature thermal properties of the binders and the resulting kinetic parameter fits. Burnham and Weese [11] developed more complex nucleation and growth degradation models, but first-order models using their Arrhenius rate parameters reproduced the experimental weight losses closely in recent Chemical TOPAZ simulations. The binders are therefore assumed to decompose according to simple first order reactions:

$$\text{Viton A} \rightarrow \text{Decomposition Products} \tag{8}$$

$$\text{Kel-F} \rightarrow \text{Decomposition Products} \tag{9}$$

$$\begin{aligned} &\text{Estane} \rightarrow^{1} \text{Products} \quad (0-42\%); \\ &\text{Estane} \rightarrow^{2} \text{Products} \quad (42-100\%) \end{aligned} \tag{10}$$

Although only the room-temperature thermal conductivities and heat capacities of the three binders were reported [11], their variations with temperature, required for time to thermal explosion modeling, are indirectly known from experimental measurements on HMX- and TATB-based PBXs [14] compared to those for pure HMX and TATB [15].

Estane, Viton A, and Kel-F are more thermally stable than HMX, and Viton A and Kel-F are more thermally stable than TATB. In previous modeling efforts [2–5], independent kinetic data for binder decomposition was not available, so chemical kinetic parameters for reactions (8)–(10) were inferred from the effects of binder concentration on experimental ODTX times to explosion assuming independent decomposition sequences. These inferred binder decomposition rates must now be replaced by the experimentally measured decomposition rates. As shown in the Results section, the measured binder

Table 3
Binder and cross-reaction parameters

Property	Estane	Viton A	Kel-F	
Density (g/cm^3)	1.18	1.8–1.9	2.02	
Heat capacity (cal/g)	0.354	0.35	0.239	
Thermal conductivity (cal/cm-s°C)	3.53e-4	5.4e-4	1.26e-4	
Heat of formation (cal/g)	950	1778	1398	
Reaction order	1	1	1	
ln Z(s^{-1})	24.82[a]	31.49	41.44	
Activation energy Ea(kcal/mol)	37.05[b]	51.82	64.84	
Cross-reaction	Order	Heat of reaction (cal/g)	ln Z (s^{-1})	Ea(kcal/mol)
HMX products + Estane	1	600	35.0	37.05
HMX products + Viton A	1	500	50.4	51.82
TATB products + Viton A	1	500	50.4	51.82
TATB products + Kel-F	1	600	55.0	64.84

[a]For fraction reacted >0.42, ln Z = 28.13; [b]For fraction reacted >0.42, Ea = 43.74.

decomposition rates cannot explain the times to explosion of HMX and TATB PBXs if the binder is assumed to decompose independently of the explosive.

The most likely explanation of the effects of these endothermic binders on the times to explosion of HMX- and TATB-based PBXs is that the intermediate explosive decomposition products react with the surrounding binder in endothermic processes that decompose binder bonds and decrease the concentrations of the intermediate products. Thus, more of the explosive must react until the binder is sufficiently decomposed to allow the concentrations of the intermediate products to increase to the levels required for the exothermic bimolecular reactions given by Eq. (4) to accelerate to thermal explosion. Estane contains carbon-hydrogen and carbon-oxygen groups; Kel-F contains carbon-hydrogen, carbon-chlorine, and carbon-fluorine bonds; and Viton A contains carbon-hydrogen and carbon-fluorine bonds that can be attacked by explosive decomposition products. Since the initial explosive decomposition reactions occur in the condensed phase and are endothermic, the resulting condensed phase intermediate products are unlikely to rapidly react with the surrounding binder. However, as gaseous reaction products begin to form in exothermic reactions, they are sufficiently mobile and excited to decompose neighboring polymeric binders. For HMX, intermediate gaseous products such as CH_2O, N_2O, HNO_2, and HCN are formed in slightly exothermic reactions and are mobile and reactive enough to cause bond breaking in adjacent polymers. It is known that formaldehyde reacts vigorously with Viton even under ambient conditions [16], but no chemical kinetic rate data are yet available. For TATB, the initial gaseous product is water [17], but eventually the TATB decomposition sequence produces intermediate species such as HCN, CO, CO_2, HNCO, and NO, which can react with polymer bonds [18].

As more becomes known about explosive and polymer decomposition mechanisms, more detailed models can be constructed, but, in this article, the cross-reaction between HMX and binder is assumed to be that of the intermediate gaseous products produced in Eq. (3) with the binder components:

$$\text{HMX Gaseous Intermediates} + \text{Binder} \rightarrow \text{Fragments} \quad (11)$$

This reaction is assumed to be first order in each reactant and endothermic with an overall heat of reaction less than the heat of formation of the binder. The carbon-chain backbone of the binder is unlikely to be attacked. The rest of the binder is probably not completely decomposed before the concentration of intermediate gaseous products becomes large enough that the very exothermic second-order reactions represented by Eq. (4) proceed rapidly. For TATB, the final gaseous products generated in reactions represented by Eq. (7) are assumed to react with the binder:

$$\text{TATB Final Gaseous Products} + \text{Binder} \rightarrow \text{Fragments} \quad (12)$$

As in Eq. (11), Eq. (12) is taken to be first order in each component. The activation energies for Eqs. (11) and (12) are taken to be equal to those of normal Estane, Kel-F, and Viton A decomposition, while the heats of reaction and frequency factors are varied to account for differing initial mass fractions of binder and initial temperature effects. The kinetic parameters for the HMX and TATB cross-reactions are listed in Table 3.

ODTX Results for HMX and TATB with Endothermic Binders

Newly measured and previously reported ODTX times to explosion for pure HMX, pure TATB, an HMX/TATB mixture, and the PBXs listed in Table 4 are presented in this section as the database for these two explosives and three binders. Other research explosive (RX) formulations have been tested, but they contain additional components whose effects on times to explosion are as yet uncertain.

Various explosive formulations employ fine and/or coarse particles of HMX and TATB. Fine explosive particles have greater surface areas than coarse particles. This additional surface area allows gaseous products to be generated faster upon heating at the surfaces of the explosive particles, which results

Table 4
Plastic bonded explosive compositions

A. HMX based			
LX-10-1	94.5% HMX	5.5% Viton A	
LX-07	90% HMX	10% Viton A	
LX-04	85% HMX	15% Viton A	
LX-14	95.5% HMX	4.5% Estane	
B. TATB based			
RX-03-AT	95.5% TATB	4.5% Viton A	
PBX 9502	95% TATB	5% Kel-F	
LX-17	92.5% TATB	7.5% Kel-F	
C. HMX/TATB based			
RX-26-AF	49.3% HMX	46.6% TATB	4.1% Estane
RX-26-AY	48.2% HMX	45.6% TATB	6.2% Viton A
RX-26-CG	49.85%HMX	40.57% TATB	9.58% Viton

in shorter times to thermal explosion. The ODTX experimental times to explosion and corresponding calculations based on the thermal and kinetic parameters listed in Table 1 for coarse and fine HMX were previously published [4]. Figure 1 shows the measured and calculated ODTX times to explosion versus inverse temperature for coarse TATB (30–60 mm particles) and ultrafine TATB (5–10 mm particles). The calculations are based on the TATB thermal and kinetic parameters in Table 2. As for HMX, the frequency factors for ultrafine TATB in the final two reactions, Eqs. (6) and (7), were increased slightly to account for greater surface area. HMX thermally explodes at all initial ODTX temperatures. However, below about 270°C, TATB does not. It slowly decomposes until the internal

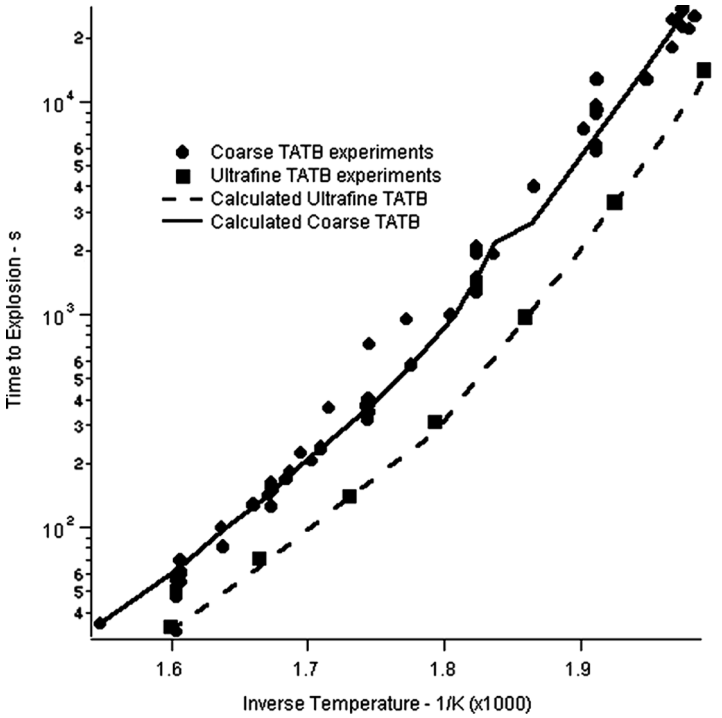

Figure 1. Experimental and calculated times to explosion for coarse and ultrafine TATB.

gas pressure exceeds the ODTX sealing pressure of 0.15 GPa, and the aluminum anvils separate without being damaged. These pressure bursts are modeled by assuming that 0.15 GPa pressure is attained when the final product concentration in Eq. (7) exceeds 5% of the total mass. As shown in Figure 1, good agreement with the TATB lower temperature ODTX data is obtained using this assumption for both coarse and fine TATB.

Figure 2 shows the experimental and calculated ODTX times to explosion for a 50% TATB, 50% HMX mixture. Large TATB particles and small HMX particles were used, so the coarse TATB and fine HMX reaction rates were used in the calculations, which agree well with the data. Calculated times

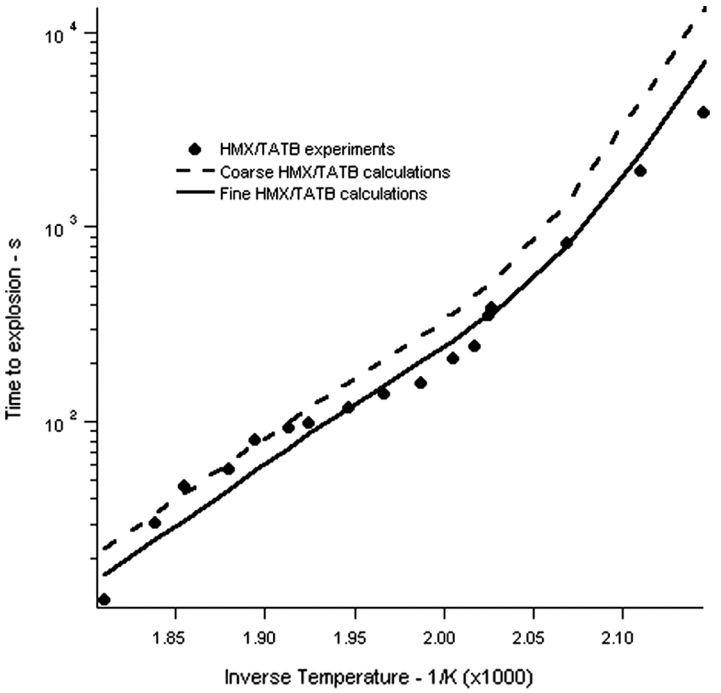

Figure 2. Experimental and calculated times to explosion for HMX/TATB.

to explosion using coarse HMX and coarse TATB parameters are also shown in Figure 2. HMX/TATB mixtures actually thermally explode at shorter times than pure HMX [2]. TATB has a higher thermally conductivity than HMX, so heat is conducted into the mixture faster than it is in pure HMX. Then the HMX in the mixture reacts sooner than it would have by itself. HMX/TATB mixtures with 40–50% HMX thermally explode at all ODTX temperatures.

The effects of endothermic binders on the ODTX times to explosion for HMX, TATB, and HMX/TATB PBXs are shown in Figures 3–5, respectively. Although there is scatter among the ODTX data points taken over the past 30 years, nearly all of the PBX times to explosion are longer than those measured for pure HMX, pure TATB, or HMX/TATB mixtures. Figure 3 contains

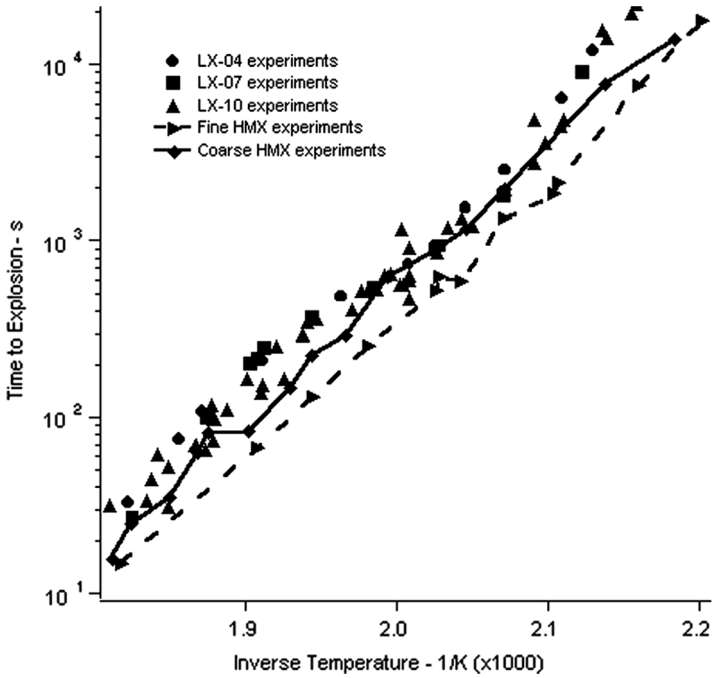

Figure 3. Experimental times to explosion for HMX/Viton A PBXs.

the ODTX data for three HMX/Viton A PBXs, LX-10-1 (5.5% Viton A), LX-07 (10% Viton A), and LX-04 (15% Viton A). Of the 72 data points for LX-10, LX-07, and LX-04 in Figure 3, only 10, which are all LX-10-1 experiments, have shorter explosion times than coarse HMX, and none have shorter times than fine HMX. These PBXs contain both coarse and fine HMX, and a pure HMX mixture of coarse and fine particle mixtures would produce an explosion time curve between those for all fine and all coarse particles. Only one temperature has been studied for the HMX/Estane explosive LX-14 (4.5% Estane), and HMX/Kel-F PBXs have not been studied. Figure 4 shows the ODTX data for two TATB/Kel-F PBXs, LX-17 (7.5% Kel-F) and PBX 9502 (5% Kel-F), and one TATB/Viton A PBX RX-03-AT (4.5%Viton A). Only two of the 32 explosion times for LX-17, PBX 9502, and RX-03-AT shown in Figure 4 are less

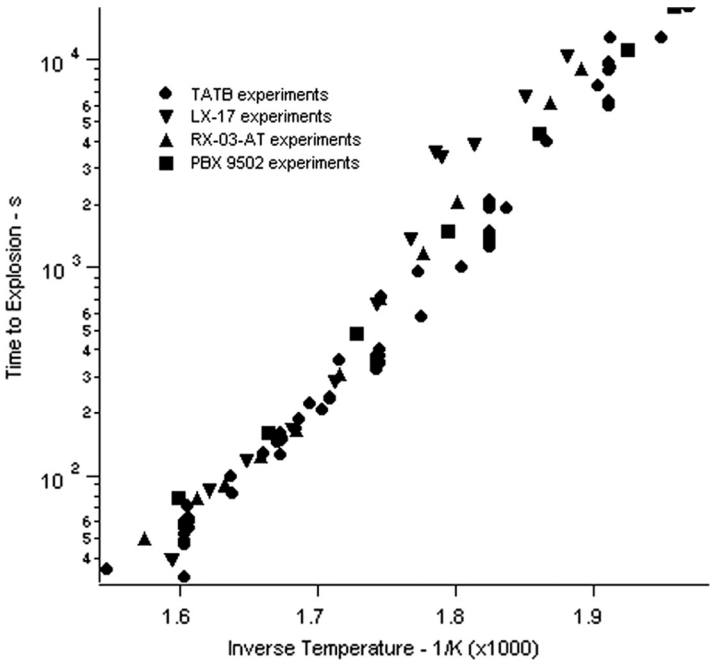

Figure 4. Experimental times to explosion for TATB PBXs.

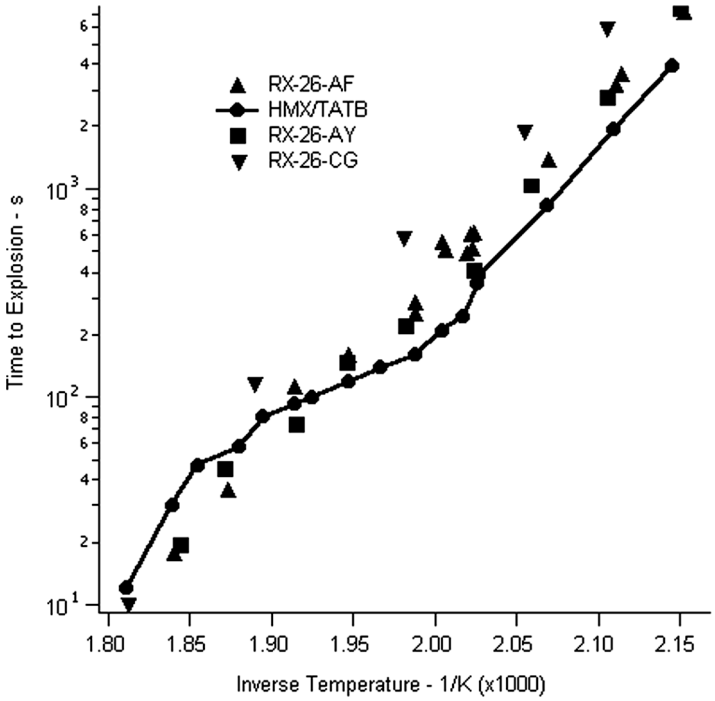

Figure 5. Experimental times to explosion for HMX/TATB PBXs.

than any of the corresponding 103 explosion times shown for pure TATB. Viton A has a greater effect on TATB explosion times than the same mass percentage of Kel-F. Figure 5 shows the ODTX data for two HMX/TATB/Viton A PBXs, RX-26-AY (6.2% Viton A) and RX-26-CG (9.6% Viton A), and one HMX/TATB/Estane PBX RX-26-AF (4.1% Estane). Five of the 30 explosion times for these HMX/TATB PBXs are less than those of pure HMX/TATB at the same temperatures, as shown in Figure 5. Estane appears to have a larger effect on explosion time than Viton A per unit mass percentage for HMX/TATB PBXs. ODTX data on LX-14 at various temperatures are required for a second comparison of the relative effects of Estane and Viton A on times to explosion of PBXs.

Comparisons of Experimental and Calculated Times to Explosion

The comparisons between calculated and experimental times to explosion are presented in this section. The ODTX times to explosion are compared to LX-04 calculations assuming that Viton A decomposes independently from HMX according to the measured kinetic rates listed in Table 3. The entire heat of formation of Viton A, 1778 cal/g, is used to maximize the endothermic effect of independent binder decomposition. Figure 6 shows the resulting ODTX curves. The calculated times to explosion are shorter than those measured for LX-04, because very little of the Viton A reacts. At most 20% of the Viton A present in LX-04 is predicted to react at the lowest

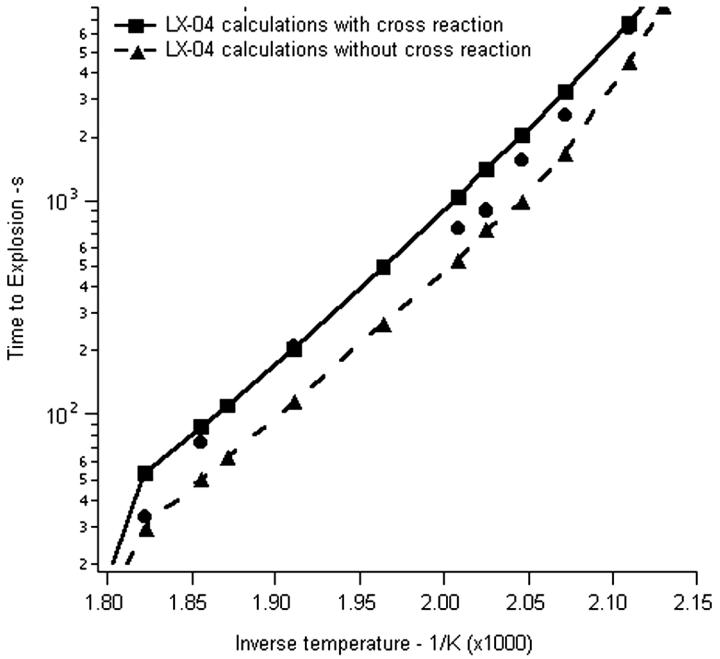

Figure 6. Experimental and calculated times to explosion for LX-04 with and without the HMX Products + Binder cross-reaction.

temperature, longest time to explosion. Thus cross-reactions between the explosive decomposition products and the binder are required to cause the observed longer times to explosion for PBXs compared to the pure explosives.

The cross-reaction parameters are listed in Table 3. Included in Figure 6 is the calculated LX-04 ODTX curve with the cross-reaction between Viton A and the HMX intermediate gaseous products. The calculated times assuming a cross-reaction with a reasonable heat of reaction (500 cal/g) agree closely with the measured LX-04 times to explosion in Figure 6. The calculated and experimental ODTX times to explosion curves for the series of three HMX/Viton A PBXs are plotted in Figure 7. Good overall agreement is obtained. The one data point for LX-14 is 914 s to thermal explosion at 498.85 K, and the calculated time is 876.15 s using the coarse HMX rates from

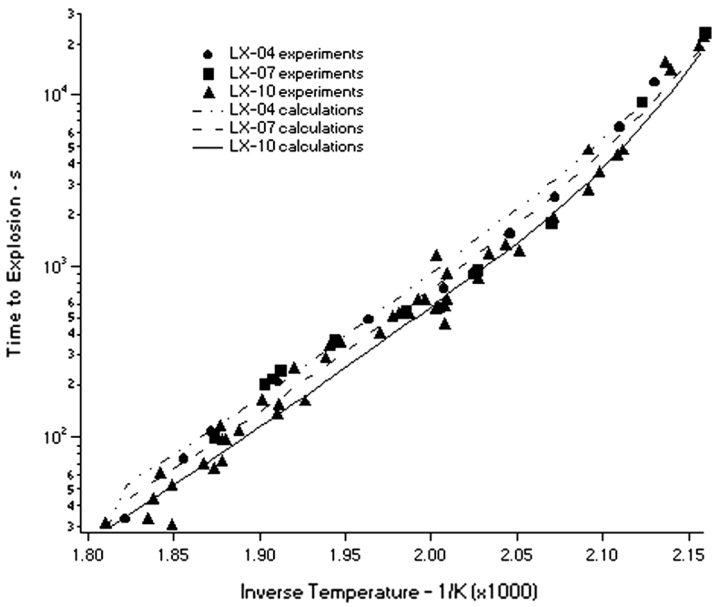

Figure 7. Experimental and calculated times to explosion for HMX/Viton A PBXs.

Table 5
Time to explosion comparisons for other experiments

Experiment	Time (s)	Cross-reactions Time (s)	% Error	Independent reactions Time (s)	% Error
A. LX-04					
ODTX	21,321	21,905	2.74	20,611	3.33
ODTX	21,172	21,775	2.85	20.436	3.48
STEX #06	303,120	295,600	2.48	258,700	14.65
STEX #07	258,480	266,800	3.22	238,840	7.60
STEX #09	333,720	338,800	1.52	310,850	6.85
STEX #10	328,680	338,800	3.08	310,850	5.42
STEX #28	357,120	351,060	1.70	321,610	9.94
STEX #29	358,920	353,190	1.60	325,240	9.38
B. LX-10					
STEX #47	246,110	248,660	1.04	237,885	3.34
STEX #51	1176	1203.2	2.31	1183.7	0.65

Table 1 and the cross-reaction rate parameters for HMX products + Estane listed in Table 3.

For HMX/Viton A PBXs, several other time to explosion experiments have been conducted and calculated. Table 5 lists the experimental and calculated times to explosion with and without cross-reactions, along with percentage errors between the experimental and the calculated times. The tests include two ramped temperature ODTX experiments on LX-04, six scaled thermal explosion (STEX) tests [19] on LX-04, and two STEX tests on LX-10-1. The overall agreement between the experimental and calculated times to explosion for LX-04 is much improved when a cross-reaction is included, especially for the very long times of the six STEX experiments. Since LX-10-1 contains less Viton A binder than LX-04, the differences in the calculated times with and without a cross-reaction are not

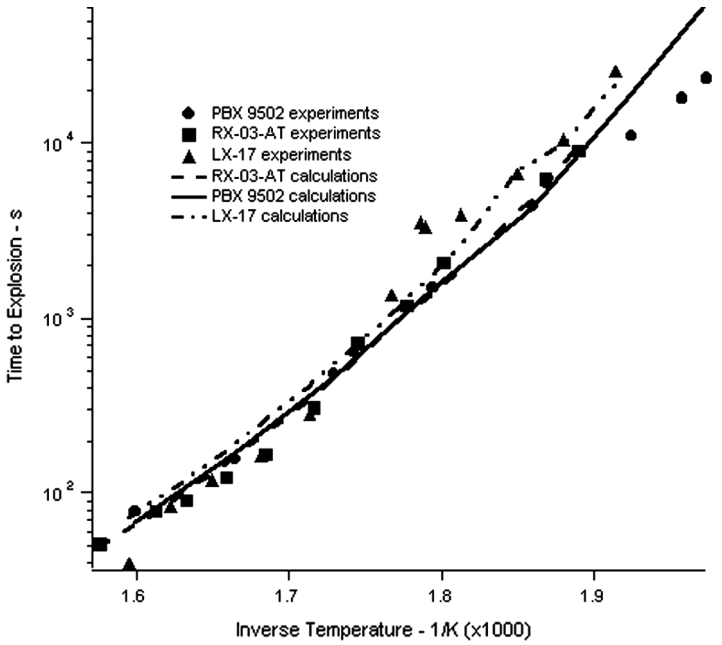

Figure 8. Experimental and calculated times to explosion for TATB PBXs.

as large as for LX-04. The calculated time for the slow LX-10 STEX experiment assuming a cross-reaction to increase Viton A decomposition agrees better with experiment than the time calculated without a cross-reaction.

For TATB-based explosives containing Kel-F and Viton A binders, the experimental and calculated ODTX curves are shown in Figure 8. The agreement between experiment and calculation for RX-03-AT, which contains 4.5% Viton A, is good. The agreement for the two TATB Kel-F PBXs, LX-17 and PBX 9502, is not quite as good. The LX-17 calculations predict low explosion times at the intermediate temperatures and correct times at the lowest temperatures, while the PBX 9502 calculations are correct at high and intermediate temperatures but high at the three lowest temperatures. This discrepancy is most likely due to the lack of knowledge concerning the rates of

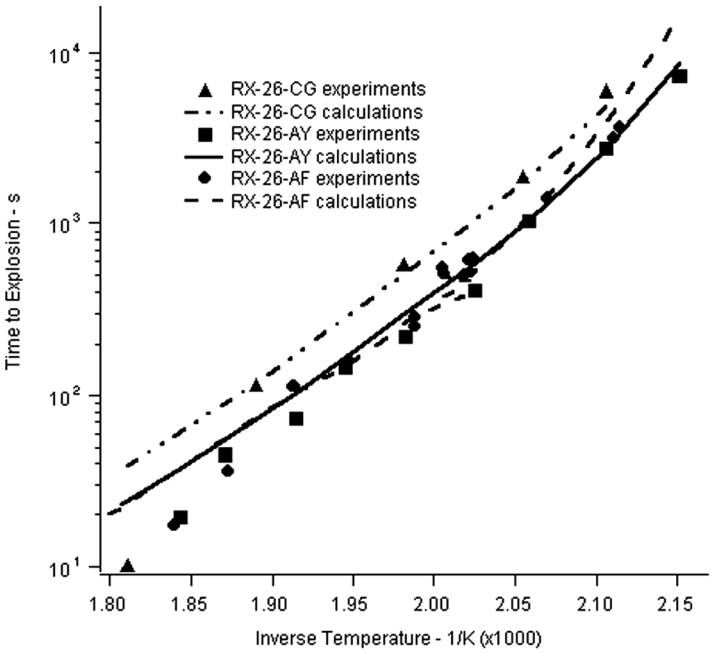

Figure 9. Experimental and calculated times to explosion for HMX/TATB PBXs.

formation of reactive, gaseous intermediate products during TATB decomposition.

For HMX/TATB PBXs, the comparisons are shown in Figure 9. The calculations for the two Viton A binder PBXs, RX-26-AY and RX-26-CG, agree well with the ODTX experimental times. The RX-26-AF calculated times agree well over most of the temperature range but are longer than experiment at the two lowest temperatures. The effect of the Estane binder in RX-26-AF is not as well understood as that of the Viton A binder. An ODTX series on LX-14 needs to be conducted to study the effects of Estane on HMX decomposition. Since HMX is the reactive explosive component in HMX/TATB PBXs, this study will also be useful for modeling HMX/TATB/Estane PBXs like RX-26-AF.

Conclusions

The ODTX and other experimental times to thermal explosion for HMX- and TATB-based PBXs are increased by the addition of the endothermic polymeric binders Estane, Viton A, and Kel-F. Decomposition reaction rates fit to the results of recent chemical decomposition experiments show that these polymers are more stable than HMX and TATB. Modeling PBX thermal decomposition using these binder kinetics and the global chemical decomposition mechanisms for HMX and TATB as independent processes cannot account for the increased times to explosion. Thus, to account for these increased times, the binders must interact with the evolving explosive decomposition products as they form. It seems likely that the binders react with the early gaseous decomposition products, because these gaseous products are more mobile and energetic than condensed phase decomposition fragments. Once sufficient quantities of the final stable gaseous products form in highly exothermic bimolecular reactions, bimolecular chain reactions between vibrationally excited products [20] rapidly lead to thermal explosion. The binder's carbon-hydrogen, carbon-oxygen, carbon-chlorine, and/or carbon-fluorine bonds are attacked by the intermediate gases, CH_2O, N_2O, HCN, and HNO_2 for

HMX and perhaps NO, HCN, HCNO, CO_2, and CO for TATB. The intermediate products are destroyed and must be regenerated. Once the neighboring binder layers are sufficiently decomposed to allow the concentrations of intermediate gases to increase the levels at which very exothermic chain reactions produce the final stable products CO_2, CO, N_2, and H_2O. The resulting rapid increases in the number of moles of gas, temperature, and pressure cause thermal explosion.

The thermal decomposition models for PBXs containing HMX, TATB, HMX/TATB, mixtures and three binders, Estane, Viton A, and Kel-F, are extended to include one cross-reaction between the postulated intermediate decomposition products of HMX or TATB and the binders. The activation energies for these cross-reactions are assumed to be equal to those fit to experimental binder decomposition data. The cross-reaction frequency factors are assumed to be higher than those fit to the measured binder decomposition rates to reflect the greater internal energy and mobility of the gaseous explosive decomposition products. The heats of reaction required for these cross-reactions to accurately calculate ODTX time versus inverse temperature curves and other experimental times to explosion are approximately 1/3 to 1/2 of the heats of formation of the binders. This implies that the binders are not decomposed down to their completely stripped carbon backbones before the thermal explosion process occurs.

Obviously, the chemical mechanisms involved in thermal explosion of solid explosives are much more complex than the three-step TATB model and the four-step HMX model used here [12]. This is also true for the steps in the degradation of the polymeric binders covering the decomposing explosive particles. The decomposition of HMX is more completely understood than that of TATB, but both require much more experimental study. Each intermediate gaseous product from explosive decomposition reacts with different bonds in the binder at different rates. An experimental program to measure the reaction rates of various explosive decomposition products with binders at high temperatures and pressures has been started [21].

The opposite binder effect, shorter times to explosion in PBXs containing exothermic binders that are less thermally stable than HMX, has been observed in some HMX-based PBXs, such as PBX 9404 (nitrocellulose binder) and PBX 9501 (BDNPA/F binder) [4]. For PBX 9404, the experimental chemical kinetic reaction rate data of Chen and Brill [22] obtained using a T-jump apparatus was used directly to model the independent decompositions of nitrocellulose and HMX under ODTX thermal explosion experimental conditions. Since the reaction products of nitrocellulose are similar to those of HMX [12], cross-reactions between the binder product gases and the heated, unreacted HMX particles are likely and will be studied. Such chemical kinetic reaction rate studies are required to begin to quantify the myriad processes involved in thermal decomposition of condensed phase explosives. The results of these experimental studies will be used to develop of more complex models of pure explosives and PBXs. With these advanced models, more complete simulations can be made of thermal explosion, impact ignition, shock initiation, and detonation processes.

Acknowledgments

The authors thank all the experimentalists who generated the ODTX and STEX data, as well as Alan Bunrham and Randall Weese for many interesting discussions. The authors also thank Dr. Melvin Baer of Sandia National Laboratories for the original suggestion of cross-reactions between explosive decomposition products and the surrounding binders. This work was performed under the auspices of the United States Department of Energy by the Lawrence Livermore National Laboratory under contract no. W-7405-ENG-48.

References

[1] Steele, R. D., L. A. Stretz, G. W. Taylor, and T. Rivera. 1989. Effects of Binder Concentration on the Properties of Plastic Bonded Explosives. *Proceedings of the Ninth Symposium (International)*

on Detonation, Office of the Chief of Naval Research OCNR 113291–7, Portland, OR, August 28, p. 1014–1018.

[2] McGuire, R. R. and C. M. Tarver. 1981. Chemical Decomposition Models for the Thermal Explosion of Confined HMX, TATB, RDX, and TNT Explosives. *Proceedings of the Seventh Symposium (International) on Detonation*, Naval Surface Weapons Center NSWC MP 82–334, Annapolis, MD, June 16, p. 56–65.

[3] Tarver, C. M., T. D. Tran, and R. E. Whipple. 2003. Thermal decomposition of pentaerythritol tetranitrate. *Propellants, Explosives, Pyrotechnics*, 28: 189–193.

[4] Tarver, C. M. and T. D. Tran. 2004. Thermal decomposition models for HMX-based plastic bonded explosives. *Combustion and Flame*, 137: 50–62.

[5] Chidester, S. K., C. M. Tarver, L. G. Green, and P. A. Urtiew. 1997. On the violence of thermal explosion in solid explosives. *Combustion and Flame*, 110: 264–280.

[6] Yoh, J. J., M. A. McClelland, J. L. Maienschein, A. L. Nichols, and C. M. Tarver. 2006. Simulating thermal explosion of octahydrotetranitrotetrazine-based explosives: Model comparison with experiment. *J. Applied Physics*, 100: 073515.

[7] Tarver, C. M. 2004. Chemical kinetic modeling of HMX and TATB laser ignition tests. *J. Energetic Materials*, 22: 93–107.

[8] Tarver, C. M., S. K. Chidester, and A. L. Nichols III. 1996. Critical conditions for impact- and shock-induced hot spots in solid explosives. *J. Phys. Chem.*, 100: 5794 –5799.

[9] Tarver, C. M. and A. L. Nichols III. 1998. Hot Spot Growth in a Thermal-Chemical-Mechanical Reactive Flow Model for Shock Initiation of Solid Explosives. *Proceedings of the Eleventh International Detonation Symposium*, Office of Naval Research ONR 33300-5, Aspen, CO, August 30, p. 599–609.

[10] Nichols III, A. L. and C. M. Tarver. 2002. A Statistical Hot Spot Reactive Flow Model for Shock Initiation and Detonation of Solid High Explosives. *Proceedings of the Twelfth International Symposium on Detonation*, Office of Naval Research ONR333-05-2, San Diego, CA, August 11, p. 489–496.

[11] Burnham, A. K. and R. K. Weese. 2005. Kinetics of thermal degradation of explosive binders Viton A, Estane and Kel-F. *Thermochimica Acta*, 426: 85–92.

[12] Behrens Jr., R., S. B. Margolis, and M. L. Hobbs. 1998. A Zero-Dimensional Model of Experimental Thermal Decomposition of

HMX. *Proceedings of the Eleventh International Detonation Symposium*, Office of Naval Research ONR 33300-5, Aspen, CO, August 30, p. 533–542.

[13] Nichols III, A. L. and K. W. Westerberg. 1993. Modification of a thermal transport code to include chemistry with thermally controlled kinetics. *Numerical Heat Transfer*, Part B, 24: 489–499.

[14] Cornell, R. H. and G. L. Johnson. 1978. Measuring Thermal Diffusivities of High Explosives by the Flash Method. *Lawrence Livermore Laboratory Report No. UCRL-52565*, October 23.

[15] Hanson-Parr, D. M. and T. P. Parr. 1999. Thermal properties measurements of solid rocket propellant oxidizers and binder materials as a function of temperature. *J. Energetic Materials*, 17: 1–30.

[16] Glascoe, E. A. 2007. *Lawrence Livermore National Laboratory*. Private communication, May 17.

[17] Sharma, J., J. C. Hoffsommer, D. J. Glover, C. S. Coffey, J. W. Forbes, T. P. Liddiard, W. L. Elban, and F. Santiago. 1985. Paramagnetic Decomposition Products from Energetic Materials. *Proceedings of the Eighth Symposium (International) on Detonation*, Naval Surface Weapons Center NSWC 86-194, Albuquerque, NM, July 15, p. 725–733.

[18] Land, T. A., W. J. Siekhaus, M. F. Foltz, and R. Behrens. 1993. Condensed-Phase Thermal Decomposition of TATB Investigated by AFM and STMBMS. *Proceedings of the Tenth International Detonation Symposium*, Office of Naval Research ONR 33395–12, Boston, MA, July 12, p. 181–189.

[19] Wardell, J. F. and J. L. Maienschein. 2002. The Scaled Thermal Explosion Experiment. *Proceedings of the Twelfth International Symposium on Detonation*, Office of Naval Research ONR333-05-2, San Diego, CA, August 11, p. 384–393.

[20] Tarver, C. M. 1997. Multiple roles of highly vibrationally excited molecules in the reaction zones of detonation waves. *J. Phys. Chem.*, 101: 4845–4851.

[21] Glascoe, E. A. 2007. *Lawrence Livermore National Laboratory*. Private communication, June 24.

[22] Chen, J. K. and T. B. Brill. 1991. Thermal decomposition of energetic materials 50, kinetics and mechanism of Nitrate Ester Polymers at high heating rates by SMATCH/FTIR Spectroscopy. *Combustion and Flame*, 85: 479–495.